

# SARS-CoV-2 RNA extraction using magnetic beads for rapid large-scale testing by RT-qPCR and RT-LAMP

Steffen Klein<sup>1,2,#</sup>, Thorsten G. Müller<sup>1,#</sup>, Dina Khalid<sup>1</sup>, Vera Sonntag-Buck<sup>1</sup>, Anke-Mareil Heuser<sup>1</sup>, Bärbel Glass<sup>1</sup>, Matthias Meurer<sup>3,4</sup>, Ivonne Morales<sup>5</sup>, Angelika Schillak<sup>1</sup>, Andrew Freistaedter<sup>1</sup>, Ina Ambiel<sup>1</sup>, Sophie L. Winter<sup>1,2</sup>, Liv Zimmermann<sup>1</sup>, Tamara Naumoska<sup>1</sup>, Felix Bubeck<sup>1</sup>, Daniel Kirrmaier<sup>3,4</sup>, Stephanie Ullrich<sup>1</sup>, Isabel Barreto Miranda<sup>1</sup>, Simon Anders<sup>3</sup>, Dirk Grimm<sup>1,6</sup>, Paul Schnitzler<sup>1</sup>, Michael Knop<sup>3,4,7</sup>, Hans-Georg Kräusslich<sup>1,6</sup>, Viet Loan Dao Thi<sup>1,2</sup>, Kathleen Börner<sup>1,6,\*</sup> and Petr Chlanda<sup>1,2,\*</sup>

1) Center of Infectious Diseases, Virology, Heidelberg University Hospital, Heidelberg, Germany

2) Schaller Research Groups, Center of Infectious Diseases, Virology, Heidelberg University Hospital, Heidelberg, Germany

3) Center for Molecular Biology of Heidelberg University (ZMBH), Heidelberg, Germany

4) German Cancer Research Center (DKFZ), Heidelberg, Germany

5) Center of Infectious Diseases, Clinical Tropical Medicine, Heidelberg University Hospital, Heidelberg, Germany

6) German Center for Infection Research (DZIF), Heidelberg, Germany

7) DKFZ-ZMBH Alliance, Heidelberg, Germany

# Equal contribution.

\* Correspondence: [petr.chlanda@bioquant.uni-heidelberg.de](mailto:petr.chlanda@bioquant.uni-heidelberg.de); [kathleen.boerner@bioquant.uni-heidelberg.de](mailto:kathleen.boerner@bioquant.uni-heidelberg.de)

---

## Abstract

Rapid large-scale testing is essential for controlling the ongoing pandemic of severe acute respiratory syndrome coronavirus 2 (SARS-CoV-2). The standard diagnostic pipeline for testing SARS-CoV-2 presence in patients with an ongoing infection is predominantly based on pharyngeal swabs, from which the viral RNA is extracted using commercial kits followed by reverse transcription and quantitative PCR detection. As a result of the large demand for testing, commercial RNA extraction kits may be limited and alternative, non-commercial protocols are needed. Here, we provide a magnetic bead RNA extraction protocol that is predominantly based on in-house made reagents and is performed in 96-well plates supporting large-scale testing. Magnetic bead RNA extraction was benchmarked against the commercial QIAcube extraction platform. Comparable viral RNA detection sensitivity and specificity were obtained by fluorescent and colorimetric RT-LAMP using N primers, as well as RT-qPCR using E gene primers showing that the here presented RNA extraction protocol can be combined with a variety of detection methods at high throughput. Importantly, the presented diagnostic workflow can be quickly set up in a laboratory without access to an automated pipetting robot.

## 1. Introduction

SARS-CoV-2, the causative agent of coronavirus disease 2019 (COVID-19) was first described in the city of Wuhan in China in December 2019 and spread globally thereafter to cause a pandemic. To slow its spread, large-scale diagnostics and the enforcement of strict public health measures were implemented in many countries. The current standard test for SARS-CoV-2 detection and diagnosis is based on viral RNA extraction from a pharyngeal swab followed by the highly sensitive reverse transcription and quantitative PCR (RT-qPCR) method. Several primer sets targeting one or more of the SARS-CoV-2 genes – N, E, S or RNA-dependent RNA polymerase (RdRp) – have been used [1]. A two-step testing procedure using primer sets targeting the E gene for initial screening followed by the RdRp gene to confirm positive samples is recommended by the German Consiliary Laboratory for Coronaviruses [2]. The unprecedented global demand for commercial RNA extraction kits and the ensuing shortage of these reagents [3], led to the establishment of several diagnostic workflows performed on patient samples with or without an intermediate RNA extraction step [4–7]. Viral RNA isolation from clinical samples depends on the rapid inactivation of viral particles, typically by detergent solubilization and on the denaturation of omnipresent RNases [8]. The latter may be accomplished by the use of chaotropic chemicals, such as guanidinium salts [9] or non-specific proteases that are active on both native and denatured proteins, such as proteinase K. In either case, after virus particle lysis, RNA must be purified since guanidinium salts, proteinase K and organic solvents inhibit the subsequent RT-qPCR step. RNA can be separated from proteins either by liquid phase separation using chloroform-aqueous emulsions after lysis with a commercially available Trizol (a mixture of guanidinium thiocyanate and acid phenol) or by means of solid-phase separation using silica [10]. Nucleic acid-binding to negatively charged silica (SiO<sub>2</sub>) is facilitated by guanidinium salts and the basic pH of the lysis buffer [11]. To achieve a high nucleic acid binding capacity, silica-based nucleic acid extraction methods use either porous silica matrices embedded in a column (spin column) [12], a tip (TruTips) [13] or a suspension of microparticles. Microparticles can be separated from the lysate either by centrifugation or by a magnetic field if the microparticles' dense iron-containing cores are coated with porous silica [14].

The protocol established in this study aimed at extracting SARS-CoV-2 RNA from respiratory patients' swabs (oropharyngeal and nasopharyngeal) and is based on the magnetic bead-based nucleic acid extraction protocol published by He *et al.* [15] and on the protocol from Chemicell GmbH, who provided the SiMAG-N-DNA magnetic beads. We opted for silica magnetic beads because of their relatively easy manufacturing and sustainable availability, and because specialized plasticware (spin columns, modified tips) is not required to perform their separation. Magnetic bead RNA extraction was performed in 96-well plates using a magnet plate optimized for 96 deep-well plates. To minimize the pipetting and handling errors, the portable manual pipetting system Liquidator 96, which is less expensive than automated pipetting robots, was used (Figure 1A). Here, we show that the magnetic bead-based protocol yields RNA extracts comparable to the commercially available QIAcube viral RNA extraction kit, as determined by the

commonly applied detection methods RT-qPCR and reverse transcription loop-mediated isothermal amplification (RT-LAMP) [16].

## 2. Materials and Methods

### 2.1 Clinical samples and sample lysis

A selection of upper respiratory tract specimens (flocked swabs in Amies medium, eSwab Copan, Brescia, Italy) sent to the diagnostics laboratory of the Heidelberg University Hospital between April and May 2020 for SARS-CoV-2 PCR were used for the study. 17 out of 77 tested positive and 60 tested negative for SARS-CoV-2 by RT-qPCR. In this study, we used samples from the same day (2 positive, 20 negative) or samples collected on previous days that were stored at -20 °C (15 positive, 40 negative). In order to facilitate replicate testing, positive samples were further diluted and used in replica to generate 88 positive and 76 negative samples.

The following steps were performed in a biosafety level 2 (BSL-2) laboratory according to standard microbiological and diagnostic practices. To extract SARS-CoV-2 RNA from pharyngeal swabs, a lysis buffer containing 5 M guanidinium thiocyanate, 40 mM dithiothreitol, 20 µg/ml glycogen, 1 % Triton X-100 and buffered with 25 mM sodium citrate to pH 8 was used. Internal control (IC) for RT-qPCR (5 µl/sample) (Tib-Molbiol, Germany) was added into the lysis buffer just before use. To ensure both rapid virus deactivation and RNase denaturation, 140 µl lysis buffer and 140 µl sample were vigorously vortexed in a 1.5 ml Eppendorf tube for 10 sec and incubated for 10 min at room temperature inside a BSL-2 laminar flow cabinet. Lysates (280 µl) were transferred into a 96 deep-well plate (Greiner AG, Austria) with a maximum working volume of 500 µl per well, which is compatible with the Liquidator 96 pipetting system.

### 2.2 RNA extraction using magnetic beads in 96-well plate format

Just before the RNA extraction, SiMAG-N-DNA magnetic beads (Chemicell, Germany) were washed three times in RNase-free water. The aqueous magnetic bead stock solution of 100 µg/µl was added into absolute ethanol to obtain a working solution of 5 µg/µl. Using a multichannel pipette, 200 µl of magnetic bead solution was transferred into the 96 deep-well plate containing the pharyngeal sample lysates. To facilitate the adsorption of the nucleic acid onto the magnetic beads, the 96-deep-well plate was placed on an orbital shaker MS3 (IKA, Germany) for 8 min at 500 – 1000 rpm, before the mixture was resuspended using a Liquidator 96, Model 200 µl (Mettler Toledo, USA) (Figure 1A,B) and placed again on the orbital shaker for additional 7 min. Subsequently the plate was placed on a magnet plate for 96-deep-well plates (Magtivio, Netherlands) (Figure 1C) for 10 min to allow the magnetic beads to form rings on the bottom of the wells (Figure 1D,E). The clear supernatant was discarded using the Liquidator 96 and magnetic beads were washed three times with 200 µl 70 % ethanol and briefly rinsed with 50 µl RNase-free water to remove any residual ethanol. Finally, nucleic acids adsorbed onto the surface of the magnetic beads were eluted into 60 µl RNase-free water. A detailed step-by-step procedure and a

complete list of all materials and instruments used for this magnetic bead RNA extraction protocol can be found in the Supplementary Data.

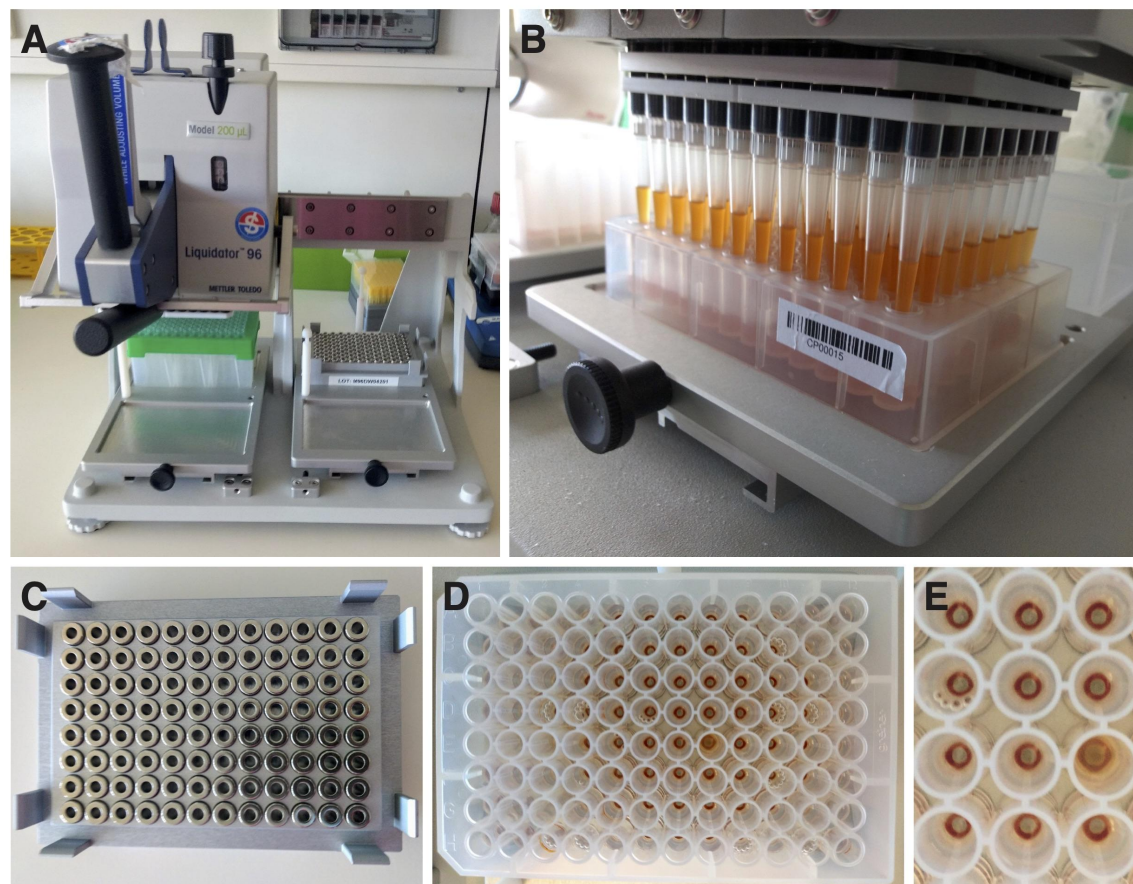


**Figure 1.** Magnetic bead RNA extraction using the Liquidator 96 pipetting system. (A) Liquidator 96, Model 200 µl. (B) The liquidator is used to resuspend magnetic beads in the 96-deep-well plate. (C) Magnet plate used to separate the magnetic beads and the supernatant. (D,E) Ring-shaped pellets are formed after placing the 96-deep-well plate onto the magnetic ring plate (C) for 10 min.

### 2.3 RNA extraction using QIAcube

To compare the performance of the magnetic bead RNA extraction, the QIAamp Viral RNA body fluid kit was carried out with manual lysis according to the manufacturer's protocol (Qiagen, Germany). The sample input volume was 140  $\mu$ l, the volume of IC per sample was 10  $\mu$ l and the elution volume was set to 100  $\mu$ l.

### 2.4 SARS-CoV-2 RNA detection by RT-qPCR

For RT-qPCR detection of the SARS-CoV-2 E gene, we adopted a widely used protocol based on Corman *et al.* [2]. For the Mastermix, 0.5  $\mu$ l of Primer/Probe LightMix® Modular SARS and Wuhan CoV E-gene (Tib-Molbiol, Berlin) and 0.5  $\mu$ l of LightMix® Modular EAV RNA Extraction Control (Tib-Molbiol, Germany) was mixed with 4.9  $\mu$ l RNase-free water, 4  $\mu$ l LightCycler® Multiplex RNA Virus Master (Roche, Switzerland) and 0.1  $\mu$ l Reverse Transcriptase Enzyme (supplied with LightCycler® Multiplex RNA Virus Master kit) per sample. The following primers and probe were used: fwd 5'-ACAGGTACGTTAATAGT TAATAGCGT-3', rev 5'-ATATTGCAGCAGTACGCACACA-3', probe FAM-ACACT AGCCATCCTTACTGCGCTTCG-BBQ. 10  $\mu$ l of Mastermix was distributed into a 96-well PCR plate and 10  $\mu$ l of purified RNA from patient samples was added using the Liquidator 96, Model 10  $\mu$ l. RT-qPCR was performed using a LightCycler® 480 Instrument II (Roche, Switzerland) with 5 min of reverse transcription at 55 °C, initial denaturation at 95 °C for 5 min and subsequent 45 amplification cycles with 95 °C for 5 sec, 60 °C for 15 sec, 72 °C for 15 sec and finally cooling to 40 °C for 30 sec. Cycle threshold (CT) was determined, where fluorescence signal of the amplification reaction was above the background fluorescence, using the LightCycler software (Roche, Switzerland). Data analysis was performed in Excel and GraphPad Prism (GraphPad Software, USA), and 95 % "exact" Clopper-Pearson confidence intervals were calculated using MedCalc (MedCalc Software, Belgium).

### 2.5 Estimation of detection limit of magnetic bead RNA extraction using MS2 RNA spike-in

Five  $\mu$ l diluted MS2 RNA (Roche, Switzerland) containing  $6.1 \times 10^1$  to  $6.1 \times 10^6$  molecules was spiked into 140  $\mu$ l lysis buffer before a 140  $\mu$ l patient sample was added. Magnetic bead RNA extraction was performed as described in section 2.2. RT-qPCR for MS2 was performed with a one-step RT-qPCR reaction (Tib-Molbiol) using the following primers and probe: fwd 5'-GAGTGTTTACAGTTCCGAA-3', rev 5'-CCCCTTTCTGGAGGTACATATTCATA-3' and probe Cy5-AATAGATCGGGCTGCCTGT AAGGAGC-BBQ. 10  $\mu$ l of RNA was used per RT-qPCR, covering a range from  $10^1$  to  $10^6$  MS2 RNA molecules per reaction.

## 2.6 SARS-CoV-2 RNA detection by RT-LAMP

RT-LAMP detection of the SARS-CoV-2 N gene was based on the protocol by Dao Thi *et al.* [6]. Per reaction, the master mix consisted of 6.25  $\mu$ l WarmStart® Colorimetric LAMP 2X Master Mix M1800 (New England Biolabs, USA) and 1.25  $\mu$ l 10x LAMP primer mix targeting the N gene [17]. Immediately afterwards, 7.5  $\mu$ l of the freshly prepared reaction mix was distributed into 96-well plates and 5  $\mu$ l of purified RNA was added using a Liquidator 96, Model 20  $\mu$ l. The plate was sealed with a transparent adhesive foil and subsequently incubated at 65 °C for 30 min in a 96-well-PCR block with heated lid (75 °C). Absorbance was measured at 434 nm and 560 nm wavelengths in a Spark® Cyto or Infinite M200 plate reader (Tecan, Switzerland). Phenol red absorbance spectra change in response to the acidification of the reaction (the absorbance at 434 nm wavelength is increased and the absorbance at 560 nm wavelength is decreased). To measure pH changes during the reaction, the difference between optical densities was calculated ( $\Delta OD = OD_{434nm} - OD_{560nm}$ ) and samples with  $\Delta OD < 0.3$  were classified as negative.

For the fluorescent LAMP assay, the master mix contained 6.25  $\mu$ l WarmStart® LAMP Kit 2X Master Mix E1700 (New England Biolabs, USA), 1.25  $\mu$ l 10x LAMP primer mix targeting the N gene [17] and 0.25  $\mu$ l of 50x fluorescent dye (Syto-9, supplied with the RT-LAMP kit). 7.75  $\mu$ l of the mix was distributed in a 96-well plate and 4.75  $\mu$ l purified RNA was added before the plate was sealed and incubated at a constant temperature of 65 °C using a LightCycler® 480 Instrument II (Roche, Switzerland). Real-time fluorescence was detected with intervals of 1 min for a duration of 90 min. Time of amplification (TOA) was determined based on a fluorescence threshold, where fluorescence signal of the amplification reaction was above the background fluorescence, using the LightCycler software. Samples with TOA > 25 min were classified as negative.

### 3. Results

The magnetic bead RNA extraction protocol was established in a 96-well plate format as part of the diagnostic workflow (Figure 2). The complete workflow from RNA extraction to RNA detection can be conducted in less than 4 – 5 hours.

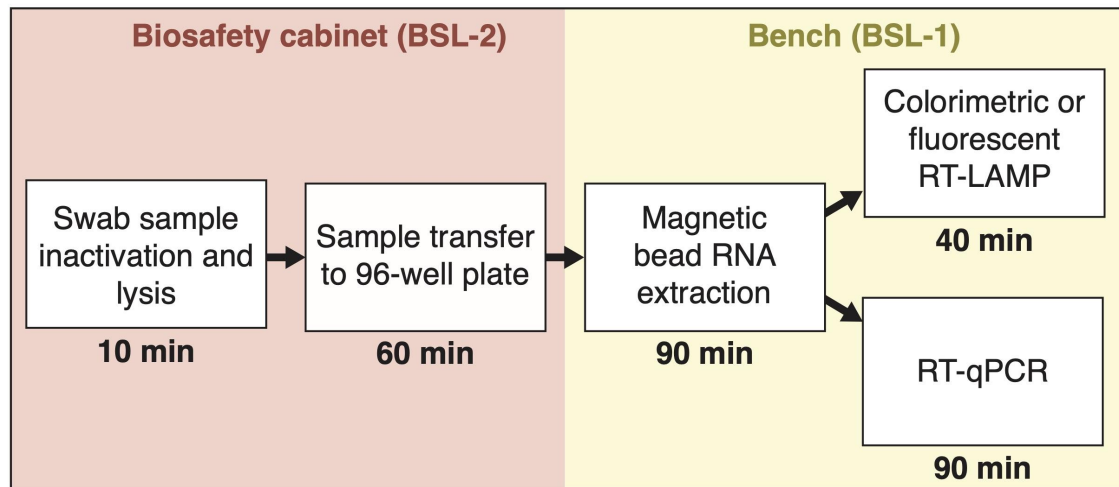


**Figure 2.** Overview and timeline of sample processing using a magnetic bead RNA purification protocol for SARS-CoV-2 diagnostics.

#### 3.1 RNA extraction using magnetic beads yields RT-qPCR results that are comparable to a commercial extraction kit

To compare the magnetic bead RNA extraction protocol with the commercial QIAcube extraction method, we first applied both protocols on one SARS-CoV-2 positive pharyngeal swab sample, which was diluted in RNase-free water prior to RNA isolation in a 10-fold dilution series up to  $10^5$  fold. The extracted RNA was subjected to RT-qPCR using E gene primers. Viral RNA was detected in samples diluted up to  $10^5$  fold after either QIAcube or magnetic bead RNA extraction (Figure 3A,C). RT-qPCR of the extracted RNA by either of the two methods showed approximately equidistant amplification curves with an interval of 4 CT values for each 10-fold dilution step (Figure 3B,D).

To further evaluate linearity of the magnetic bead RNA extraction method across a broad range of defined RNA inputs, a dilution series of RNA from MS2 bacteriophage was added to the swab sample prior to magnetic bead RNA extraction and subjected to RT-qPCR using MS2 primers (Figure 3E,F). CT values were linear over five orders of magnitude with a goodness of fit of  $R^2 = 0.9804$ . The lower limit of detection ( $\sim$  CT 40) was less than 10 RNA copies/reaction (Figure 3E).

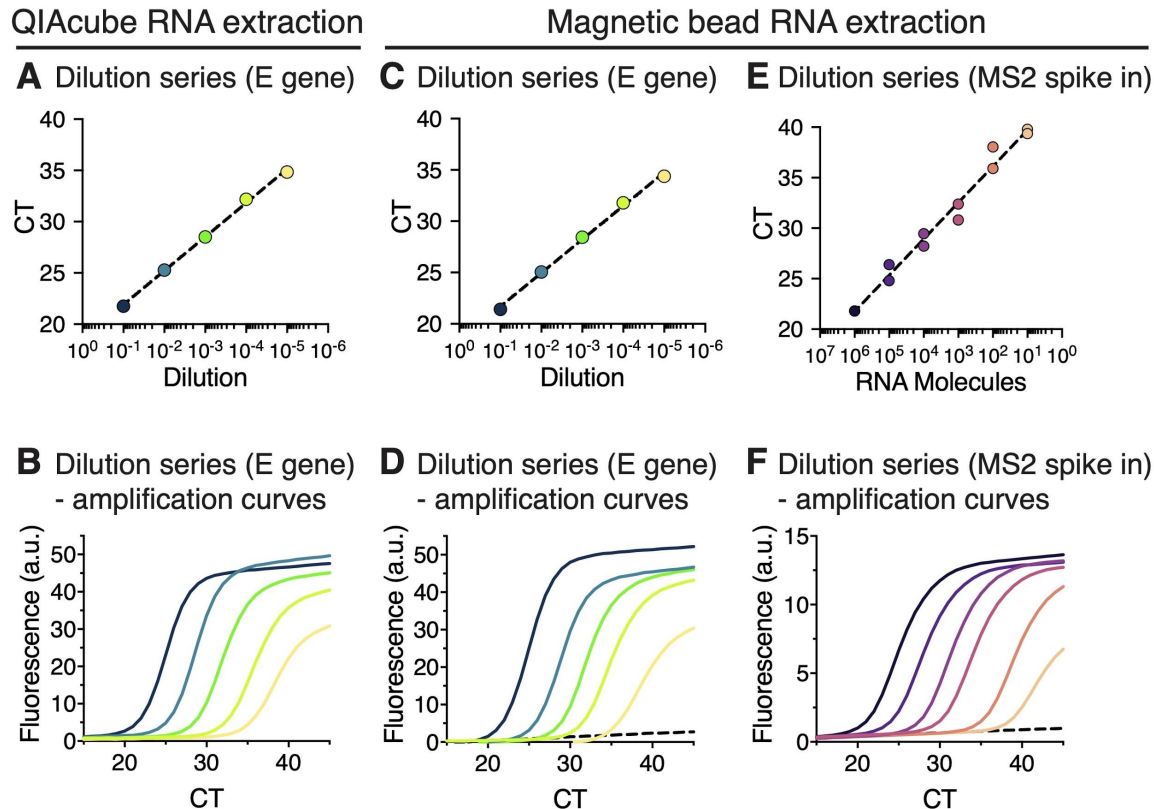


**Figure 3.** RT-qPCR of RNA extracted from sample dilution series using either the QIAcube RNA extraction kit or the magnetic beads RNA extraction. (A-D) One positive patient sample was diluted in a 10-fold dilution series from  $10^1$  to  $10^5$  fold (dark blue – green – yellow). (A) RT-qPCR CT values of RNA extracted using the QIAcube RNA extraction protocol shown on a semi-logarithmic scale. Semilog non-linear regression shows a goodness of fit of  $R^2=0.998$ . (B) RT-qPCR amplification curves of RNA extracts shown in (A); a.u., arbitrary units. (C) RT-qPCR CT values of RNA extracted using the magnetic bead RNA extraction protocol shown on a semi-logarithmic scale. Semilog non-linear regression shows a goodness of fit of  $R^2=0.996$ . (D) RT-qPCR amplification curves of RNA extracts shown in (C). Dashed black line shows an undiluted RNA sample from a SARS-CoV-2 negative patient. (E,F) Analysis of linearity and detection sensitivity of magnetic bead RNA extraction protocol using MS2 RNA spike-in. Dilution series of MS2 RNA from  $10^1$  to  $10^6$  (black – purple – orange), was added into SARS-CoV-2 positive patient samples prior to magnetic bead RNA extraction. (E) CT values for each dilution (duplicates) were plotted against calculated molecule numbers of MS2 RNA per RT-qPCR reaction on a semi-logarithmic scale. Shown are all data points and the semilog non-linear regression with a goodness of fit of  $R^2 = 0.980$ . (F) RT-qPCR amplification curves of diluted MS2 RNA extracts shown in (E) for one duplicate. Dashed black line is a sample without MS2 spike-in.



### *3.2 RT-qPCR performed on magnetic bead extracted RNA shows a high detection sensitivity and specificity*

To evaluate the magnetic bead RNA extraction protocol on larger sets, 88 SARS-CoV-2 positive and 76 negative samples generated from upper respiratory tract patient specimens were subjected to three independent magnetic bead RNA extractions as well as to QIAcube extractions. CT values of 82 positive samples obtained by RT-qPCR using primers for the E gene and IC values from either magnetic bead or QIAcube extraction were compared. In the remaining 6 samples, CT values for E gene were not detected after magnetic bead RNA purification but detected CT values for IC confirmed successful RNA extraction. Noteworthy, all six samples were previously frozen and had a CT value higher than 35 as determined by RT-qPCR after the QIAcube RNA extraction. The E gene CT values obtained from the magnetic bead and QIAcube RNA extraction were in good agreement as shown by the goodness of the linear fit of  $R^2 = 0.967$  (Figure 4A). The average IC CT of 29.3 (SD = 1.2, n = 82) after magnetic bead extraction were the same as compared to the average IC CT of 29.3 from the QIAcube RNA extractions (SD = 2.3, n = 82) (Figure 4B,C), showing that the magnetic bead RNA extraction protocol is robust.

Since assays performed in a 96-well plate format can be prone to cross-contaminations, we evaluated the sensitivity and specificity of the three independent magnetic bead RNA extractions. Samples were randomly distributed in interspaced groups of positive and negative samples on the 96-well plate. CT values below 40 obtained by RT-qPCR from QIAcube extracted RNA were used as cutoff for true positives. Rates of true and false positives in the RT-qPCR after magnetic bead RNA extraction were calculated accordingly. Eighty-two samples were identified as true positives and 73 as true negatives, while three samples were classified as false positives and six as false negatives yielding a sensitivity and specificity of 93 % (95 % confidence intervals (CI): 86 – 97 %) and 96 % (95 % CI: 93 – 100 %), respectively (Figure 4D, Supplementary Table 1). With a CT cutoff of 35, we did not detect any false negatives resulting in a sensitivity of 100 % (95 % CI: 95 – 100 %), showing that false negatives were samples with high CT values and the negative results are rather due to fluctuation of the viral load around the limit of detection and unlikely a result of cross contamination.

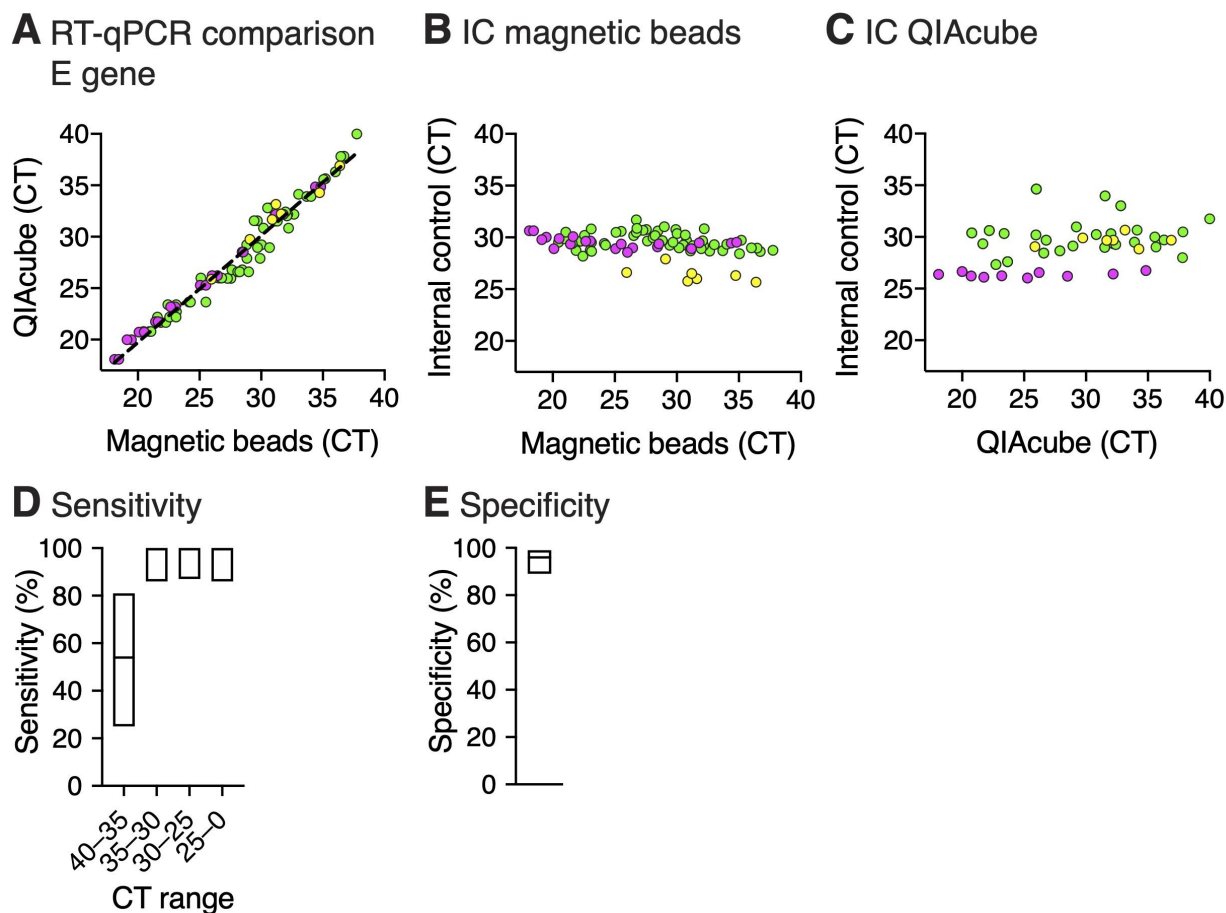


**Figure 4.** RT-qPCR of RNA extracted from SARS-CoV-2 positive patient samples using magnetic bead RNA extraction and QIAcube RNA extraction. RNA extraction was performed on three sets of SARS-CoV-2 positive patient samples with a total sample number of 82 (yellow = 7 samples, magenta = 20 samples, green = 55 samples) in parallel with either the magnetic bead RNA extraction protocol or the automated QIAcube extraction kit and further analyzed by RT-qPCR using the E gene. **(A)** Comparison of RT-qPCR analysis of RNA extracted by the two different extraction methods. Plot shows the E gene CT values for each sample. A linear regression ( $R^2 = 0.967$ ) is plotted as a dashed line. **(B,C)** Analysis of the internal control of the RT-qPCR for RNA extracted by the magnetic bead RNA extraction protocol **(B)** or QIAcube extraction kit **(C)**. Plots show the CT values of the internal control plotted against the E gene CT values. **(D,E)** Sensitivity **(D)** and specificity **(E)** analyzed by RT-qPCR of the three independent magnetic bead RNA extractions. To determine sensitivity and specificity, QIAcube RT-qPCR results were used as a reference. RT-qPCR after magnetic bead RNA extraction provides close to 100 % sensitivity and specificity at a cutoff CT of 35. Data is shown as mean with indicated 95 % Clopper-Pearson confidence intervals (Supplementary Table 1).

### 3.3 RNA extraction using magnetic beads is compatible with the RT-LAMP assay

Due to shortages in RT-qPCR reagents, we also recently explored RT-LAMP assay as a valid alternative RNA detection method [6]. We compared the standard pipeline QIAcube RNA extraction followed by E gene RT-qPCR detection with magnetic RNA extraction followed by RT-LAMP detection using primer sets targeting the N gene, with either colorimetric (Figure 5A – C, Supplementary Table 2) or fluorescent (Figure 5D – F, Supplementary Table 3) read-out. In total, we tested RNA extracted from 52 positive and 29 negative pharyngeal clinical samples.

During DNA synthesis, the formation of a phosphodiester bond results in release of a molecule of pyrophosphate and a proton causing a gradual acidification of the reaction mix. The detection principle of colorimetric RT-LAMP is based on monitoring pH changes during the DNA amplification, which occurs only in positive samples. Typically, phenol red, which changes color from red to yellow when the pH is lowered, is used as a pH indicator [18]. The color change can be determined by measuring the difference between the wavelengths of the two absorbance maxima of phenol red. As shown in Figure 5A, the majority of isolated RNA samples with a CT  $\approx$  30 value obtained from RT-qPCR using the E gene, yielded a color change with  $\Delta$ OD values between 0.3 and 0.4. Therefore, we used a  $\Delta$ OD value of 0.3 as a threshold for positive samples. The majority of samples with higher CT values, especially between CT 35 and CT 40, scored negative ( $\Delta$ OD < 0.3), while all negative RT-qPCR samples also scored negative in the RT-LAMP assay. Using a CT cutoff of 30, the overall sensitivity of the colorimetric assay with magnetic bead-isolated RNA was 97 % (95 % CI = 83 – 100 %) (Figure 5B), with a specificity of 100 % (95 % CI = 88 – 100 %) (Figure 5C).

The fluorescent RT-LAMP assay is based on a fluorescent dye that intercalates into amplifying DNA strands, allowing their detection in real time. Magnetic bead isolated samples with CT  $\approx$  30 led to a fluorescent signal at early time points (approx. 20 – 25 min) as compared to negative samples (> 40 min). Therefore, we used the time point 25 min as a threshold for positive samples. Similar to the colorimetric read-out, the majority of samples with higher CT values, especially between CT 35 and CT 40, scored negative (> 40 min) (Figure 5D). All negative RT-qPCR samples also scored negative (> 70min). Using a CT cutoff of 30, the overall sensitivity of the fluorescent assay was 100 % (95 % CI = 88 – 100 %) (Figure 5E), with a specificity of 100 % (95 % CI = 88 – 100 %) (Figure 5F).

These results are in agreement with the recently reported sensitivity cutoff at CT 30 for the RT-LAMP assay [6] and thus confirm that RNA purified by the presented magnetic bead extraction is compatible with RT-LAMP detection without lowering its sensitivity.

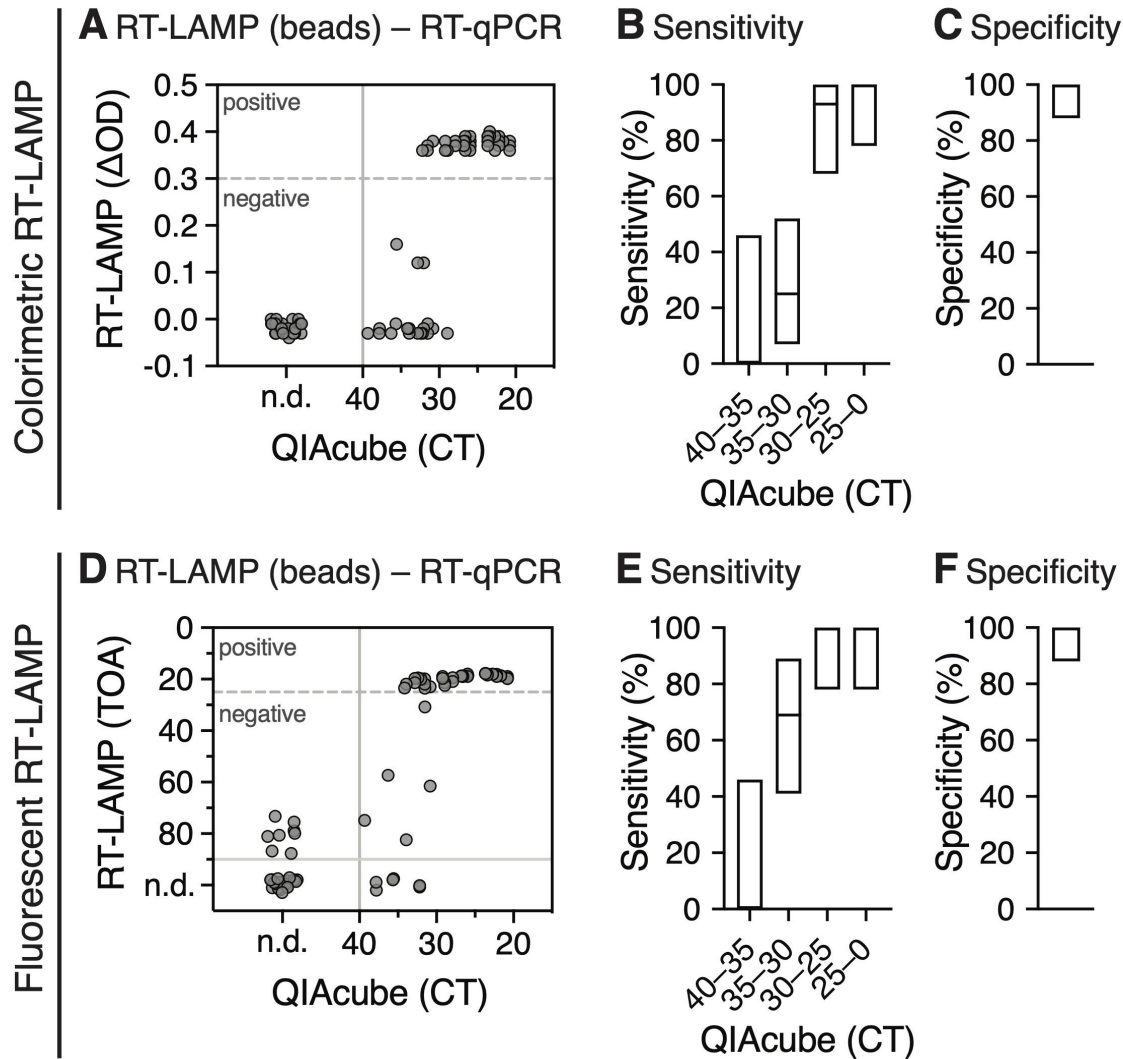


**Figure 5.** Analysis of colorimetric (A – C) and fluorescent (D – F) RT-LAMP on RNA extracted using the magnetic bead RNA extraction protocol compared to RT-qPCR CT values obtained from RNA isolated by the QIAcube extraction. (A) Scatter plot shows optical density differences obtained from colorimetric RT-LAMP ( $\Delta OD = OD_{434nm} - OD_{560nm}$ ) at a time point of 30 min. The  $\Delta OD$  threshold of 0.3 is indicated as a dashed line. All samples with a CT > 40 were considered as negative (solid line); n.d., not determined. (B,C) Sensitivity (B) and specificity (C) of colorimetric RT-LAMP for different CT ranges. The boxes indicate the 95 % Clopper-Pearson confidence interval (Supplementary Table 2). (D) Scatter plot shows time of amplification (TOA) in min for each sample obtained from fluorescent RT-LAMP compared to RT-qPCR CT values obtained from RNA isolated by the QIAcube extraction. The TOA threshold of 25 min (dashed line) was used to define positive and negative samples from RT-LAMP. All samples with a CT > 40 and TOA > 25 min were considered as true negative (solid lines). (E,F) Sensitivity (E) and specificity (F) of fluorescent RT-LAMP for different CT ranges. The boxes indicate the 95 % Clopper-Pearson confidence interval (Supplementary Table 3).

## 4. Discussion

Within the last decades, the frequency of emerging virus outbreaks has increased globally [19,20], possibly as a result of cumulative anthropogenic environmental changes that increase the risk of zoonotic transmission [21]. Due to globalization, many of the outbreaks have an increased pandemic potential and pose a burden on society and health systems. The currently ongoing SARS-CoV-2 pandemic emphasizes the urgency of appropriate preparedness and response. Before a therapeutic or vaccine exists, the early identification and isolation of positive patients remains the most effective way to inhibit further human-to-human spread and mitigate the disease outbreak. In case of a respiratory viral disease, such as influenza or COVID-19, pharyngeal swabs are collected and tested for the presence of viral RNA. RNA isolation prior to detection is a pivotal step to ensure high specificity and sensitivity of detection methods. To this end, robust and high-throughput nucleic acid isolation methods with high manufacturing and distribution capacity must be available. However, the majority of commercially available RNA purification kits are cost-ineffective and often rely on multiple components that are not easily replaceable, and their supply can often not be guaranteed. In addition, buffer compositions are not provided. Thus, overall, commercial kits do not offer enough flexibility and availability when it comes to a large epidemic or a pandemic.

Here, we provide a magnetic bead-based RNA extraction protocol that is to a large extent producer independent, does not rely on unique components that are difficult to replace and is scalable for mass testing. Because of the large surface binding capacity and rapid separation in solution by magnetic field, silica coated magnetic beads are compatible with a variety of plasticware and can be used in high throughput multiwell format [15,22] as well as in small scale testing [15]. In addition, magnetic beads can be prepared from widely available chemicals in a laboratory with basic equipment [23]. Recently, a magnetic bead RNA purification protocol has been established for automated, high throughput SARS-CoV-2 diagnostics by the COVID-19 Crick Consortia [22]. However, to carry out the protocol, a sophisticated infrastructure is required, and the protocol is partially dependent on commercial buffers. Our aim was to provide a robust protocol that can be rapidly implemented and carried out in most of the laboratories around the world equipped with a magnetic plate, a multichannel pipette or with a manual 96 pipetting device. We established a magnetic bead RNA isolation protocol that takes approximately 90 minutes using a single 96-well plate as part of a workflow for SARS-CoV-2 diagnostic. The rate-limiting and the most labor-intensive step of the presented workflow is the sample transfer from swab tubes to 96-well plates. Special care should be taken regarding sample handling prior to RNA isolation, and samples should be kept at 4 °C and processed during the day of collection. A single freeze-thawing cycle of a SARS-CoV-2 positive swab sample results in decreased sensitivity of RT-qPCR by approximately 5 CT values (data not shown). In contrast to other magnetic bead based nucleic acid purification protocols [15,22], which rely on an air-drying step to remove residual ethanol before elution, we rinse magnetic beads with a small amount of RNase-free water. Introduction of this step made our protocol more robust since air-drying in a 96-well plate is slow and uneven. Furthermore, air-drying did not lead to complete removal of ethanol, which interfered with the

subsequent RT-qPCR even at low concentrations. We report a similar RNA extraction yield compared to the commercial QIAcube extraction kit and validate that the quality of the RNA extract is suitable for RT-qPCR and RT-LAMP detection. RT-LAMP relies on a different DNA polymerase than RT-qPCR and thus provides a supplier-independent alternative to RT-qPCR. Additionally, RT-LAMP is faster and cheaper compared to RT-qPCR and does not require a thermocycler [6]. Although it is possible to perform RT-qPCR [24,25] and RT-LAMP on unpurified patient samples [6,26], the combination with our magnetic bead RNA extraction protocols increases the sensitivity. Due to the low cost, high-throughput compatibility and independence from sophisticated laboratory equipment like automated RNA extraction kits and RT-qPCR machines, the combination of magnetic bead RNA extraction and RT-LAMP offers a framework for diagnostic preparedness in case of mass-scale testing.

In conclusion, we report a detailed step-by-step RNA extraction protocol from pharyngeal swabs which is based on magnetic beads and does not depend on commercial extraction kits and reagents. Our protocol was validated in 96-well plate format by the detection of SARS-CoV-2 RNA by RT-qPCR and RT-LAMP and provides reliable RNA extraction for a diagnostic pipeline that can be rapidly deployed during the SARS-CoV-2 pandemic and is also accessible to regions with insufficient laboratory capacities. This might be of importance in case of possible future shortages of commercial RNA extraction kits and enables diagnostic labs to be well prepared in case of a new rise of SARS-CoV-2 cases. Our protocol can be easily adapted to fully automated liquid handling robotic systems and is very likely suitable for isolation and downstream detection assays for any kind of RNA virus isolated from pharyngeal swabs.

**Author contributions:** Conceptualization, MK, H-GK, VLDT, KB, PC; methodology, SK, TGM, DK, VS-B, AMH, BG, MM, AS, AF, IA, SLW, LZ, TN, FB, SU, VLDT, KB, PC; validation, SK, TGM, VLDT, KB, PC; formal analysis, SK, TGM, IM, VLDT, KB, PC; investigation, SK, TGM, DK, VS-B, AMH, BG, MM, IM, AS, AF, IA, SLW, LZ, TN, FB, SU, IBM, SA, DG, PS, MK, H-GK, VLDT, KB, PC; writing – original draft preparation, SK, TGM, VLDT, KB, PC; writing – review and editing, SK, TGM, DK, BG, IM, VLDT, KB, PC; visualization (figures), SK, TGM; supervision, MK, H-GK, VLDT, KB, PC; project administration, BG; funding acquisition, MK, H-GK, VLDT, PC. All authors have read and agreed to the published version of the manuscript. **Funding:** This research was funded by a research grant from the Chica and Heinz Schaller Foundation (Schaller Research Group Leader Programme) to PC, VLDT, SLW and AF; by the Deutsche Forschungsgemeinschaft (DFG, German Research Foundation), project number 240245660 – SFB 1129 to PC, SK, VLDT, DG and H-GK; and by the German Center for Infection Research (DZIF TTU HIV 04.815) to DG, H-GK and KB.

**Ethics statement:** The presented work was done with the intention to support SARS-CoV-2 diagnostics and improve emergency preparedness and response for COVID-19. Pseudo-anonymized surplus material from samples that had been collected for clinical diagnostics of SARS-CoV-2 were used to establish and validate the protocol presented here. This work complies with the German Act concerning the Ethical Review of Research Involving Humans, permitting use of patient samples collected to perform the testing in question, for development and improvement of diagnostic assays.

**Acknowledgments:** We thank all diagnostics employees for their technical support and advice. We thank Dr. Jan-Philipp Mallm, Prof. Dr. Karsten Rippe and Dr. Vladimir Benes for advice on magnetic bead nucleic acid purification and for lending us their instruments. We would also like to acknowledge Susanne Horner und Fabian Finger for IT support. We would like to thank different institutes on Heidelberg campus for providing devices and their employees for support, namely in alphabetical order: Prof. Dr. Johannes Backs, Nina Beil, Dr. Marco Binder, Dr. Dr. Christine Engeland, Dr. Holger Erfle, Prof. Dr. Stefan Fröhling, Dr. Richard Harbottle, Joshua Hartmann, Prof. Dr. Christel Herold-Mende, Dr. Angret Joester, Dr. Dominik Niopek, Simon John Ogrodnik, Dr. Katrin Pfütze, Dr. Steffi Sandke, Prof. Dr. Claudia Scholl, Dr. Rolf Warta, Ellen Wiedtke.

**Conflict of interest:** The authors declare no conflicts of interest.

## References

1. Vogels, C.B.F.; Brito, A.F.; Wyllie, A.L.; Fauver, J.R.; Ott, I.M.; Kalinich, C.C.; Petrone, M.E.; Casanovas-Massana, A.; Muenker, M.C.; Moore, A.J.; et al. Analytical sensitivity and efficiency comparisons of SARS-CoV-2 qRT-PCR primer-probe sets. *Infectious Diseases (except HIV/AIDS)* 2020.
2. Corman, V.M.; Landt, O.; Kaiser, M.; Molenkamp, R.; Meijer, A.; Chu, D.K.; Bleicker, T.; Brünink, S.; Schneider, J.; Schmidt, M.L.; et al. Detection of 2019 novel coronavirus (2019-nCoV) by real-time RT-PCR. *Euro Surveill.* **2020**, *25*.
3. Akst, J. RNA Extraction Kits for COVID-19 Tests Are in Short Supply in US. *The Scientist Magazine* 2020.
4. Aitken, J.; Ambrose, K.; Barrell, S.; Beale, R.; Bineva-Todd, G.; Biswas, D.; Byrne, R.; Caidan, S.; Cherepanov, P.; Churchward, L.; et al. Scalable and Resilient SARS-CoV-2 testing in an Academic Centre. *medRxiv* **2020**.
5. Guruceaga, X.; Sierra, A.; Marino, D.; Santin, I.; Nieto-Garai, J.A.; Bilbao, J.R.; Lorizate, M.; Aspichueta, P.; coBIG (COVID19 Basque Inter-institutional Group); Mayor, U. Fast SARS-CoV-2 detection protocol based on RNA precipitation and RT-qPCR in nasopharyngeal swab samples. *Infectious Diseases (except HIV/AIDS)* 2020.
6. Dao Thi, V.L.; Herbst, K.; Boerner, K.; Meurer, M.; Kremer, L.P.M.; Kirrmaier, D.; Freistaedter, A.; Papagiannidis, D.; Galmozzi, C.; Klein, S.; et al. Screening for SARS-CoV-2 infections with colorimetric RT-LAMP and LAMP sequencing. *Infectious Diseases (except HIV/AIDS)* 2020.
7. Zhao, Z.; Cui, H.; Song, W.; Ru, X.; Zhou, W.; Yu, X. A simple magnetic nanoparticles-based viral RNA extraction method for efficient detection of SARS-CoV-2. *Molecular Biology* 2020, *727*.
8. Lever, M.A.; Torti, A.; Eickenbusch, P.; Michaud, A.B.; Šantl-Temkiv, T.; Jørgensen, B.B. A modular method for the extraction of DNA and RNA, and the separation of DNA pools from diverse environmental sample types. *Front. Microbiol.* **2015**, *6*, 476.
9. Chomczynski, P.; Sacchi, N. The single-step method of RNA isolation by acid guanidinium thiocyanate-phenol-chloroform extraction: twenty-something years on. *Nat. Protoc.* **2006**, *1*, 581–585.
10. Boom, R.; Sol, C.J.; Salimans, M.M.; Jansen, C.L.; Wertheim-van Dillen, P.M.; van der Noordaa, J. Rapid and simple method for purification of nucleic acids. *J. Clin. Microbiol.* **1990**, *28*, 495–503.
11. Vandevanter, P.E.; Lin, J.S.; Zwang, T.J.; Nadim, A.; Johal, M.S.; Niemz, A. Multiphasic DNA adsorption to silica surfaces under varying buffer, pH, and ionic strength conditions. *J. Phys. Chem. B* **2012**, *116*, 5661–5670.
12. Borodina, T.A.; Lehrach, H.; Soldatov, A.V. DNA purification on homemade silica spin-columns. *Anal. Biochem.* **2003**, *321*, 135–137.
13. Holmberg, R.C.; Gindlesperger, A.; Stokes, T.; Brady, D.; Thakore, N.; Belgrader, P.; Cooney, C.G.; Chandler, D.P. High-throughput, automated extraction of DNA and RNA from clinical samples using TruTip technology on common liquid handling robots. *J. Vis. Exp.* **2013**, e50356.
14. Lee, A.H.F.; Gessert, S.F.; Chen, Y.; Sergeev, N.V.; Haghiri, B. Preparation of iron oxide silica particles for Zika viral RNA extraction. *Heliyon* **2018**, *4*, e00572.
15. He, H.; Li, R.; Chen, Y.; Pan, P.; Tong, W.; Dong, X.; Chen, Y.; Yu, D. Integrated DNA and RNA extraction using magnetic beads from viral pathogens causing acute respiratory infections. *Sci. Rep.* **2017**, *7*, 45199.
16. Notomi, T.; Okayama, H.; Masubuchi, H.; Yonekawa, T.; Watanabe, K.; Amino, N.; Hase, T. Loop-mediated isothermal amplification of DNA. *Nucleic Acids Res.* **2000**, *28*, E63.
17. Zhang, Y.; Odiwuor, N.; Xiong, J.; Sun, L.; Nyaruaba, R.O.; Wei, H.; Tanner, N.A. Rapid Molecular Detection of SARS-CoV-2 (COVID-19) Virus RNA Using Colorimetric LAMP. *Infectious Diseases (except HIV/AIDS)* 2020.
18. Tanner, N.A.; Zhang, Y.; Evans, T.C., Jr Visual detection of isothermal nucleic acid amplification using pH-sensitive dyes. *Biotechniques* **2015**, *58*, 59–68.



19. Jones, K.E.; Patel, N.G.; Levy, M.A.; Storeygard, A.; Balk, D.; Gittleman, J.L.; Daszak, P. Global trends in emerging infectious diseases. *Nature* **2008**, *451*, 990–993.
20. Smith, K.F.; Goldberg, M.; Rosenthal, S.; Carlson, L.; Chen, J.; Chen, C.; Ramachandran, S. Global rise in human infectious disease outbreaks. *J. R. Soc. Interface* **2014**, *11*, 20140950.
21. Lindahl, J.F.; Grace, D. The consequences of human actions on risks for infectious diseases: a review. *Infect. Ecol. Epidemiol.* **2015**, *5*, 30048.
22. Crick COVID-19 Consortium Scalable and robust SARS-CoV-2 testing in an academic center. *Nat. Biotechnol.* **2020**.
23. Oberacker, P.; Stepper, P.; Bond, D.; Hipp, K.; Hore, T.; Jurkowski, T. Simple Synthesis of Functionalized Paramagnetic Beads for Nucleic Acid Purification and Manipulation. *BIO-PROTOCOL* **2019**, *9*.
24. Wee, S.K.; Sivalingam, S.P.; Yap, E.P.H. Rapid direct nucleic acid amplification test without RNA extraction for SARS-CoV-2 using a portable PCR thermocycler. *Microbiology* **2020**, 306.
25. Smyrlaki, I.; Ekman, M.; Lentini, A.; Vondracek, M.; Papanicolaou, N.; Aarum, J.; Safari, H.; Muradrasoli, S.; Albert, J.; Högberg, B.; et al. Massive and rapid COVID-19 testing is feasible by extraction-free SARS-CoV-2 RT-qPCR. *Infectious Diseases (except HIV/AIDS)* **2020**.
26. Rabe, B.A.; Cepko, C. SARS-CoV-2 Detection Using an Isothermal Amplification Reaction and a Rapid, Inexpensive Protocol for Sample Inactivation and Purification. *Infectious Diseases (except HIV/AIDS)* **2020**.